AIAA 2003-7044

# SUPERSONIC INLET WITH PYLONS SET AND STAR-SHAPED FOREBODY FOR MIXING, COMBUSTION AND THRUST ENHANCEMENT

**M. Gilinsky, A.L.Gonor, V.A.Khaikine**

**Hampton University, Hampton, VA**

**I.M. Blankson**

**NASA Glenn Research Center, Cleveland, OH 44135**

AIAA 12-th INTERNATIONAL SPACE PLANES AND HYPERSONIC SYSTEMS AND TECHNOLOGIES CONFERENCE
15-19 DECEMBER, 2003, NORFOLK, VIRGINIA, USA

# Supersonic Inlet with Pylons Set and Star-Shaped Forebody for Mixing, Combustion and Thrust Enhancement

**M. Gilinsky*, A.L. Gonor**, V.A. Khaikine*****
Hampton University, VA
**I.M. Blankson+**
NASA Glenn Research Center, OH

## I. ABSTRACT

Two new approaches are discussed in this paper for application in the Scramjet inlet of an air-breathing propulsion system: 1) In the first approach, the pylon set is installed in the rectangular inlet near the cowl front edge. For a quasi-axisymmetric inlet, a similar set is installed along the Star-shaped forebody axis. This set contains 3 – 4 airfoil-shaped strips or cross-sectional rings depending on the type of inlet. The inlets: rectangular, axisymmetric or star-shaped, are located at different distances from the forebody. Fuel injection takes place through these pylons, which provides for uniform mixing downstream. The locations, sizes and angles of these pylons are very important for efficient application. Optimal values of geometrical parameters were determined from multi-parametric NSE-based numerical simulations of the laminar and turbulent external/internal flows. These simulations have shown significant benefits for mixing, combustion and thrust of the proposed approach by comparison with traditional well-known designs. Experimental tests will be conducted soon at the NASA LaRC and Institute of Mechanics at Moscow State University. Preliminary estimates are very promising.

2) In the second approach, a set of traditional (ramp) injectors is installed on the backside and/or lateral side of the star-shaped forebody. Prospects of such a forebody for mixing, combustion and thrust enhancement are discussed in detail. Experimental tests for the second design are also planned.

## II. INTRODUCTION

A new concept for the scramjet inlet with ramp injector system was presented by Marble et al[1]. The dynamics of a helium jet with this type of injector are displayed in Fig. 1 ($p_i/p_a$=1, $M_i$ =1.7). In the crossflow section, the strong uplift of the jet is apparent. The paper also contains an estimation, which shows that, for equivalence ratio equal 1 (stoichiometric mixture), the injectant must be mixed into an area approximately 15 times the area of the injector nozzle. Penetration on that order would be expected, according to our calculations, by x= 1.52m yielding too long of an inlet.

The modified ramp injector, called a "swept ramp injector", was later developed by Donohue et al.[2] (Fig. 2). It is interesting to compare data on the injectant mole fraction distribution for the ramp injector and swept ramp injector. It turns out that the swept ramp injector with small orifice area (d=2.7mm) is much more effective in terms of fuel penetration within the inlet flow compared with the ramp inlet design proposed by Marble et al. [1].

---

* Research Professor, Senior AIAA Member
** Professor-Consultant
*** Research Assistant
\+ Senior Scientist, Associate Fellow AIAA

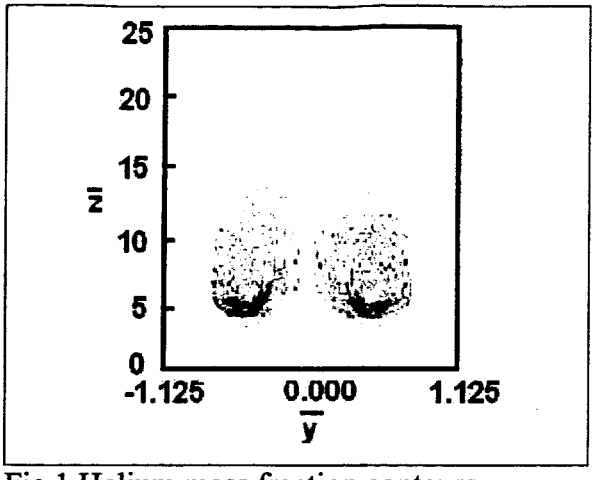


Fig.1 Helium mass fraction contours (Experimental results from [1]).

As a criterion, the ratio of the cross sectional area filled by fuel to injector orifice area was taken. This parameter for the swept ramp injector surpasses that for the ramp injector for similar conditions by 5 times. It thus appears that reduction of injector diameter (as opposed to the swept angle) contributes to the main enhancement of the fuel mixing process.

Recently a series of papers dedicated to the so-called cantilevered ramp injector was published by Sislian et al.[3-4] Its primary difference from the standard ramp injector is the significant angle of elevation of the injector axis relative to the velocity vector of the free stream flow (~$10^0$). According to the data presented, the value of the above mentioned criterion in this case is 2.83 which is slightly higher than for the standard ramp injector, 2.34. However these numbers are much lower compared with the Donohue et al. [2] swept injector.

An interesting series of works on the wall injector with non-circular orifice was published by Schetz et al.[5] According to the test results[5], the diamond-shaped orifice with sweep-back-angle of 60° generates a jet having maximum penetration height (H/d ~ 5-6) for free stream $M_\infty = 3$ and $p_{0i}/p_{0a} = 2$.

This maximum height slightly increases with yaw angle ~ $15^0$. The comparison of performance of this injector with that for a swept ramp injector allows concluding that their efficacy in terms of penetration in the free stream flow is the same.

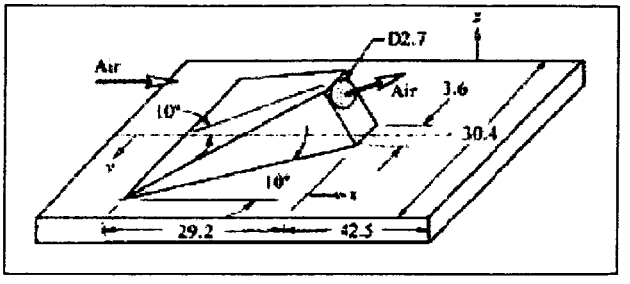


Fig.2 Schematic of the Donohue swept ramp injector [2]; all dimensions are measured in millimeters unless otherwise specified.

However, the fuel mass fraction for the wall injector in vicinity of the wall is too high (Figure 3). This fact may lead to premature combustion at the inlet wall.

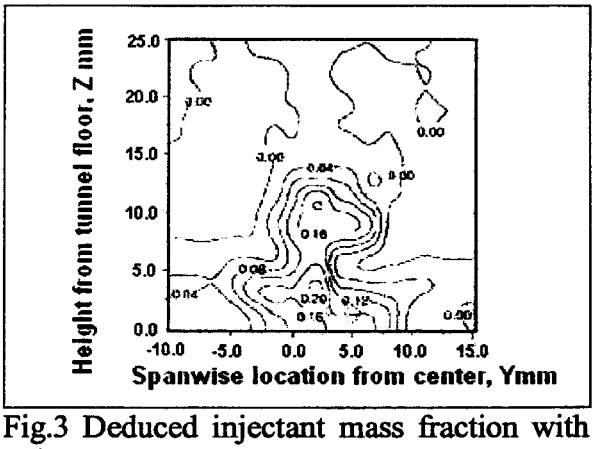


Fig.3 Deduced injectant mass fraction with 60° sweep-back angle; contours at cross section, X=110mm.

It is to be noted that, in the injector systems presented, the area (spots) with fuel distribution inside the exit section of the inlet, located at a distance of ~ 1m from the injector, makes up only 17-25 % of the total inlet exit area. A further advanced inlet

concept ([6]) with numerous additional injectors set on internal cowling surfaces undoubtedly improves the mixing process before the combustion chamber. However the core flow inside the inlet contains no injectant in this case.

Inhomogeneous fuel distribution in the existing inlet designs is caused mainly by air inflow through the bow shock wave (Figure 4) which does not interact with the fuel plume and presses it to the wall. The primary idea for mixing improvement is to bring the injectors to the flow core, as used in the "telescope inlet" (see chapter III) and an alternative possible version using "star-shaped backside injection" (see chapter IV).

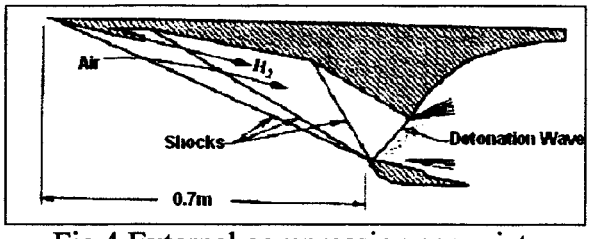


Fig.4 External compression scramjet schematic.

## III. TELESCOPE DESIGNS FOR MIXING, COMBUSTION AND THRUST ENHANCEMENT

The first new approach for application in the Scramjet inlet of an air-breathing propulsion system uses the idea of inserting several internal designs into the nozzle or inlet with locations similar to the Telescope tube containing several moving forward portions. For inlet application, the pylon set is installed in rectangular inlets near the cowl front edge whereas for the quasi-axisymmetric inlet they are installed along the Star-shaped forebody axis. Previously, this approach was applied for improvement of supersonic nozzle thrust augmentation (see [7-11]).

**3.1 Telescope Nozzle:** A divergent flow can act on a plate or airfoil inserted into a flow so that the resulting force is directed against the flow. This effect is used for thrust by supersonic nozzles. Conversely, a uniform flow produces only drag for bodies and airfoils. Inserting a conical or wedge-shaped nozzle inside the divergent part of an external nozzle produces increased thrust because the integral of the pressure on the low side of the inserted surface becomes greater than on the upper side. There is an optimal angle of the plate that provides the maximum thrust at each point of a divergent flow. The most efficient internal design is produced from a pattern that looks like a telescope with extending tubes. The optimal number of internal designs is defined through dependence on the Mach number at the nozzle exit, $M_e$. Telescoping designs must be located so that the compressible waves formed by interaction of the flow would be passed onto the upper side of the next lower telescoping part. The best result will be produced by such a set if the external design inclination increases downstream. Computations show ([7,8]) that a significant thrust benefit from the Telescope nozzle occurs with an external telescoping design, using either wedge, conical or optimal contour shapes, and also in the case of a plug application. Several designs were tested using the Kryko-Godunov marching numerical scheme and corresponding code ([12]) based on the Euler equations. The thrust calculations for the Telescope nozzle with one to four internal designs have shown that the benefits can be increased with several internal design applications. Their locations and angles to the thrust direction should be so chosen that each shock wave formed at the lower side of the upper design would not intrude upon the upper side of the lower design. Similarly, each rarefaction wave formed at the upper side of the lower design should not intrude upon the lower

side of the upper design. Thrust benefits from telescoping designs can be obtained up to ~100% and even higher when compared with the traditional wedge or conical nozzle having non-optimal angles, and up to ~30% when compared with these nozzle designs having optimal angles.

Several Telescoping designs were tested using the code developed at the Institute of Mechanics at Moscow State University (IM/MSU). This code is based on the full Navier-Stokes equations for two gas-phase models ([13]). In the second case, pure air nozzle-jet flow, the model of a chemically frozen nitrogen-oxygen stoichiometric mixture with equilibrium excitation of internal degrees of freedom is used. For the premixed hydrogen-air mixture exhausted from a divergent supersonic nozzle to the supersonic co-flow, the simplest non-equilibrium model of seven components $H_2$, $O_2$, $N_2$, $H_2O$, O, H, and OH with eight chemical reactions is employed. Comparison of results obtained from NSE and the inviscid approximation for the same configuration shows minimal thrust benefit reduction. The thrust benefit is only ~5-7% of the friction influence for the very close thrust values at Reynolds number, $Re=10^6$. This Reynolds number is calculated on the basis of critical (sound) parameters.

**3.2 Telescope Inlet:** The nontraditional nozzle design discussed above for a supersonic nozzle can also be employed for supersonic inlet improvement. The Telescope nozzle design and all results of theoretical analysis of this concept are useful for the inlet as well. In this case, the energy of the flow along the forebody wall can be used for creation of additional thrust. As in the previous analysis, the mutual locations, sizes and angles of the internal plates (thin airfoils) are very important for efficiency of the application. Optimal values of geometric parameters were determined by employing multi-parametric numerical simulations based on the modified marching K-G code ([12]). The effect of four thin airfoils installed at the minimal cross section (near the corner point) is illustrated in Figure 5. Here Mach contours and corresponding streamlines are shown for the 2D Telescope inlet with a wedge forebody. This design provides a forebody drag reduction of 25%. Obviously, the same approach is applicable for other designs, such as transition sections inside variable cross section supersonic tunnels, blunt bodies with several ring-shaped sheets, etc.

**3.3 Supersonic Inlet Containing Pylon Set:** The defects of the traditional single pylon application in a supersonic propulsion system before a combustion chamber are well known. They include: (i) appearance of an additional drag component in the flow, and (ii) increased length of the mixing layer downstream in order to provide the uniform mixture across the combustion chamber. The proposed Telescope inlet allows elimination of these defects because the specific pylon locations and their appropriate number can lead to thrust augmentation and simultaneously create 3 – 4 mixing layers across the duct which favors more effective mixing in smaller distances. That favors larger premixed media for stationary detonation and pulse detonation engines' realization. Several numerical simulation tests were conducted to examine the Telescope inlet concept for mixing and combustion improvement. The NASA VULCAN ([14]) code based on the full Navier-Stokes equations for two gas-phase models was employed. Hypersonic flight conditions with Mach number, $M_\infty=4$ and 6 were analyzed, for the same geometric inlet configuration as in the half-duct combustor problem as described above.

The pylons had thin airfoil shapes formed by two circular arcs of the same length. The heights, $h_1$, of these segments were significantly less than the airfoil chord, $L$, $(h_1/L=5\%)$. Several locations of the hydrogen fuel injectors on the pylons were analyzed: *i)* at the pylon back edge where fuel was injected through small sound nozzles with critical cross section height $h_2$, so that $h_2/L=1\%$. *ii)* Discrete or uniform distribution of fuel injection on the pylon upper side surface. *(iii)* a similar distribution of fuel injection on the pylon lower side surface. and *iv)* Discrete or uniform distribution of fuel injection on both upper and lower side surfaces. Mixing, combustion and thrust efficiencies were compared for the same total mass flow rates and total pressure of injected fuel in the different cases. The fuel static pressure was several times larger than local air pressure, and the fuel temperature at the exit was verified in the range: 300-1000°K.

The main numerical simulation tests were conducted for the 2D pylons shown in Figure 5 and Figure 6.

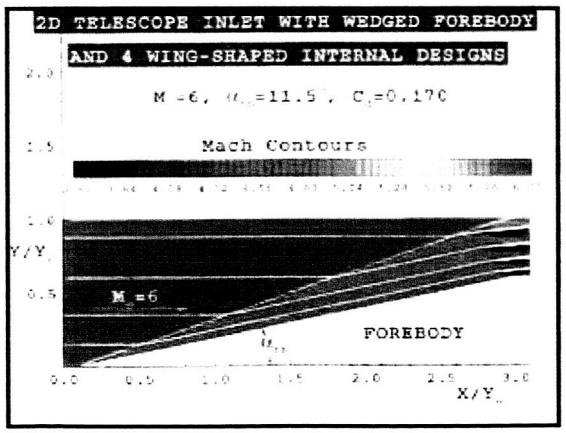


Fig.5 2D Telescope inlet with wedged forebody, 4 wing-shaped internal designs, and free stream Mach number, $M_\infty$=6.

Experimental tests will be conducted soon at the NASA LaRC and Institute of Mechanics at Moscow State University (IM/MSU). In the first stage, only cold tests for free stream Mach number, $M_\infty$=4, will be conducted at the NASA LaRC Mach 4 Blowdown facility (M4BDF). The appropriate model manufactured at the Hampton University Aeropropulsion Center is shown in Figure 7. Analogous tests for Mach number 3.5 will be conducted in the supersonic wind-tunnel, A-7, and for some 2D and quasi-axisymmetric designs at the IM/MSU hypersonic wind tunnel GAU for free stream Mach number, $M_\infty$=6. An example of the quasi-axisymmetric design, i.e. scramjet inlet with star-shaped forebody and pylon set, is shown in Figure 8.

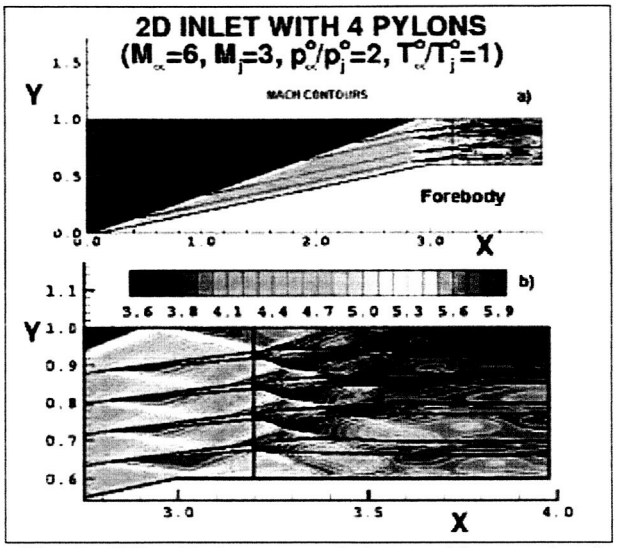


Fig.6 2D Telescope inlet with wedged forebody, 4 wing-shaped pylons, and free stream Mach number, $M_\infty$=6; injection is from pylon back side; numerical simulation based on K-G marching scheme ([12]).

Several numerical simulation tests for the 2D Scramjet inlet shown in Figure 7 were conducted for hydrogen injection from the pylon set shown for free stream Mach number, $M_\infty$=4. The simulations were based on a full NSE (elliptical) and marching approximations using the NASA VULCAN code ([14]). Some numerical results are illustrated in Figures 9, 10. These results confirm promising prospects for pylon set

applications by comparison with the traditional approaches, such as ramp sweep-back injectors located on the combustion chamber walls or cavities at the walls.

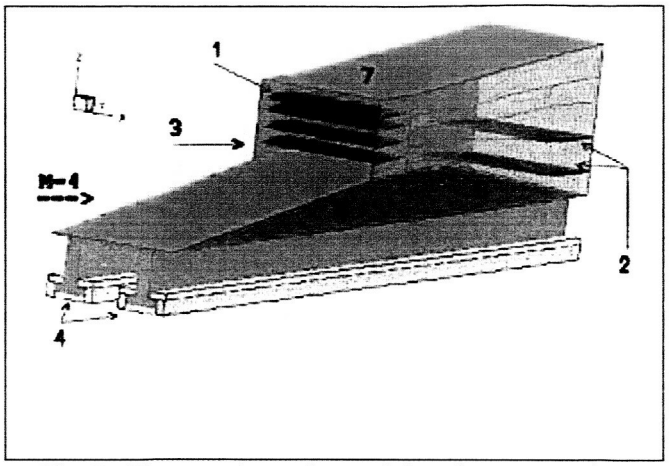


Fig.7 The projected model of rectangular Scramjet inlet and divergent wedged nozzle with 4 pylons and 2 thrusters: 1-pylons; 2-thrusters; 3- inlet; 4- moving holders for drag/thrust measurement; 5- forebody; 6-nozzle; 7- cowl.

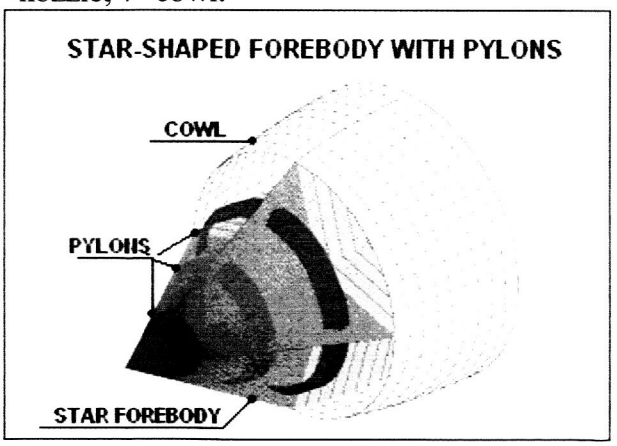


Fig.8 Scramjet inlet with Star-shaped forebody and 3 ring-shaped pylons; this design will be tested experimentally at the IM/MSU hypersonic wind tunnel, GAU, for free stream Mach number, $M_\infty$=6.

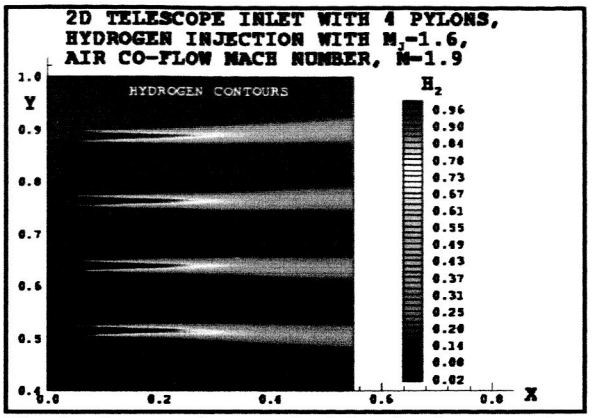


Fig.9 Interaction of 2D hydrogen jets exhausted from 4 pylons to the 2D air co-flow. Mj = 1.6; Mair=1.9; NPR=1. Numerical simulation results are based on NASA VULCAN code.

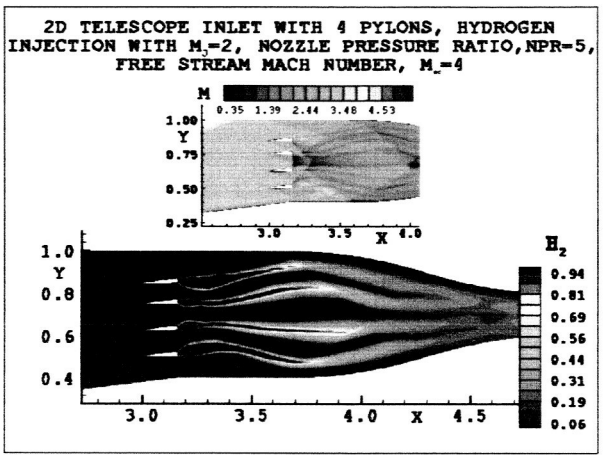


Fig.10 2D Telescope inlet with 4 pylons. Upper picture is Mach contours, and lower is hydrogen fraction contours. Hydrogen jets exhausted from pylons under different angles: two upper under $\alpha$=-60°, and two lower under $\alpha$=60°. Free stream air Mach number, $M_\infty$=4.0, and hydrogen jet Mach number, Mj = 2.0; nozzle pressure ratio, NPR=5.

## IV. SCRAMJET STAR-SHAPED INLET WITH BACK- AND/OR LATERAL-SIDE INJECTORS

**4.1 Star-Shaped Body Characteristics.** Inhomogeneous fuel distribution in the existing inlet designs is caused mainly by air

inflow through the bow shock wave (Figure 4) which does not interact with the fuel plume and presses it to the wall.

The primary idea for mixing improvement, to bring the injectors to the flow core as used in the "telescope inlet", may be also realized in the following star-shaped inlet design depicted in Figure 11.

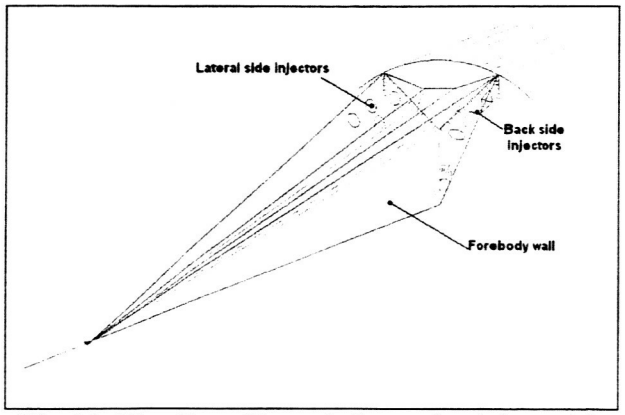


Fig.11 The Star-Shaped Scramjet inlet with back- or/and lateral- side injectors. Only one cycle is shown.

Actually this design is a modification of the axisymmetric inlet in which a conical forebody is replaced by a star-shaped body with n similar petals. The external edge of each petal stretches out to a cowl. An array of injectors is set in the rear part of the petals in order for the whole airflow between the neighbouring petals to be percolated through the cloud of the fuel formed by the injectors. It is supposed that the injector has a design similar to that presented in Ref. [5] with an elliptic or diamond orifice. By giving various sweepback and yaw angles to each injector, one can increase the penetration height of the injectant between the petals. The petal cross-section profile is fitted so that the bow shock wave is attached to the petal edges. The Mach shock wave system, accompanied by numerous weak internal shocks, should form in a cross-flow section, as seen in Figure 11.

It is well known ([15-28]) that a star-shaped body at hypersonic speed has a lesser total drag compared with the equivalent cone. These experiments made it possible to determine the values of the total drag of the model of the "star" and the cone. Star-shaped models with four and six petals arranged symmetrically relative to the longitudinal axis of the model were tested at Mach numbers $M_\infty$ = 2.53, 4.01, 5.96, and 7.74. A six-petal model is shown in Figure 12.

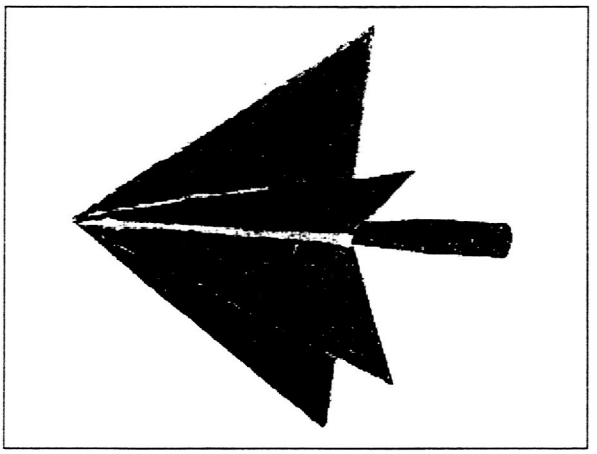

Fig.12 Six-petal model of a "star-shaped" body.

The results of balance tests on these models with 4 and 6 petals and the equivalent cone are given in Figure13. In a wide range of Mach number, from low supersonic speeds to hypersonic speeds, star-shaped bodies have significantly lower drag than an equivalent cone.

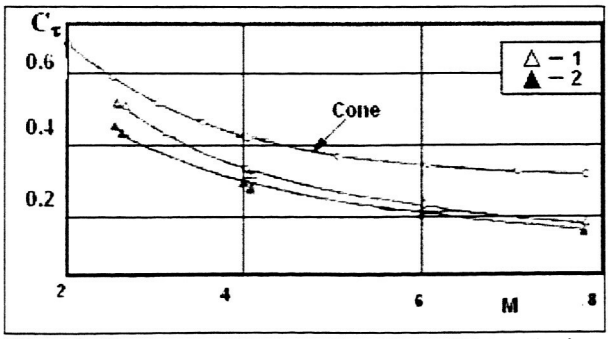


Fig.13 Drag coefficient for four (1) and six (2) petal "star-shaped" bodies and cone for

different free stream Mach number. Drag is measured by the balance system.

**4.2 Analysis of Results Relevant to a Star-Shaped Scramjet Inlet.** Now let us turn to the description of the tests that allow estimation of the possibility of the application of a star-shaped body as the scramjet inlet forebody in terms of reducing the inlet drag compared with that for a conical forebody. The fact is that, in a real scramjet system ([6]), the angles at the vertex of the cone are within the range of $10^\circ \leq \Theta \leq 20^\circ$. The values of the aspect ratio, $\lambda = L/2R$, (L – cone length, R – cone midsection radius) for such cones are in the range $1.37 \leq \lambda \leq 2.5$. Due to this, the following test results ([26-28]) presented in Figure 14 are relevant.

First of all, it is important to find the principal parameter providing a reduction in the drag as compared with a circular cone. For equivalent length L and midsection area S, this parameter was found to be the ratio of the minimum radius of the transverse contour of the star-shaped body to the radius of the cross section of the equivalent cone at the base: $r' = r / R$ (see Figure 14, top). The number of cycles n of the star-shaped body is not of fundamental importance for the minimization of the aerodynamic drag, according to Ref. [26], if r' is given (in what follows the prime has been omitted). In Figure 14, the experimental data at Mach number $M_\infty = 6$ for the drag coefficient, $c_\tau$, of star-shaped bodies at an angle of attack $\alpha = 0$ is presented. Here, n = 3, 4, and 6 cycles (a, b, and c, respectively) and r = 0.6, 0.5, and 0.4 (solid curves 1, 2, and 3). Values for the equivalent cone (broken curve in Figure 14) are also presented as a function of aspect ratio.

When $M_\infty = 6$, all the star-shaped bodies in the range of variation of the design parameters $\lambda$, r, and n considered, have a lower aerodynamic drag than the equivalent cone. When $r \in [0.4; 0.6]$ and $\lambda = 1.3$, the aerodynamic drag of the optimum star-shaped body is approximately half the drag of the equivalent cone and when $\lambda = 2$ it is less than the drag of the equivalent cone by a factor of 1.3. These data, together with the results of other studies, show that the minimum value of the ratio of the aerodynamic drag of star-shaped bodies to the $c_\tau$ of the equivalent cone is reached at Mach numbers $M_\infty > 6$.

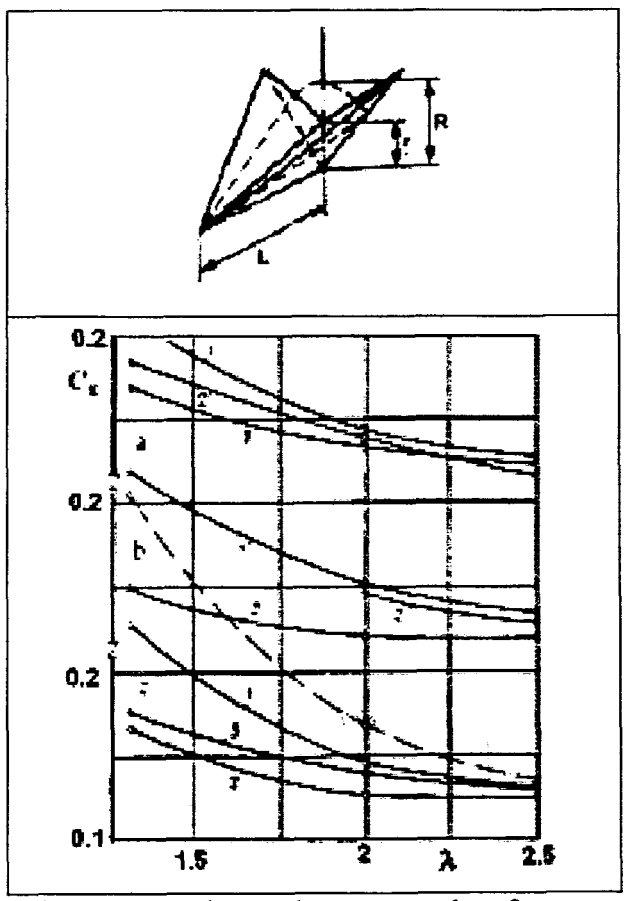


Fig.14 Experimental test results for star-shaped bodies with 3, 4 and 6 petals (a, b and c, respectively). Drag coefficient, $C_\tau$ , vs velocity coefficient, $\lambda$ (1; 2 and 3 are for r/R-0.6; 0.5 and 0.4 respectively) is presented.

It is to be noted that measurements of the dynamic pressure field in the wake of a star-

shaped body ([29,30]) were conducted using a Pitot probe. The results of the experiment showed that the coefficient of dynamic pressure recovery is higher on the tested V-shaped wings ("star" cycle) than in the optimum plane inlet with oblique plus normal shock. However it still appears to be far from the optimum value, which can be achieved by a special choice of the geometric parameters and number of petals.

**4.3 Advanced Design of Scramjet Inlet with Star-Shaped Forebody.** The preliminary design with four petals and cowling (shown in Figure 15 for one body cycle) is analyzed below with the purpose of determining the optimal conditions for DE application.

The model dimensions in Figure 15, normalized with respect to inlet entrance radius, correspond to the following values of the characteristic parameters: $r/R = 0.6$ and $\lambda = 2$. The feature of this inlet design is extension of the branched bow shock in the internal inlet and its interaction with the cowl surface (Figure 15, dash line). It is necessary that the entire inflow in the inlet pass through the bow shock.

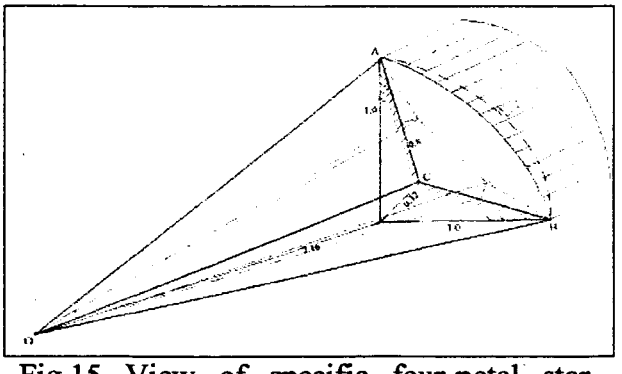

Fig.15 View of specific four-petal star-shaped inlet given for dimensions corresponding to $r/R=0.6$ and $\lambda=2$.

This condition requires that the bow shock behind the petals' butt-ends appears to be without distortion up to reflection from the cowl. The preliminary estimation produced has shown that, for the inlet model with the given geometry, displayed in Figure 15, the characteristics (rarefaction waves) coming from trailing edges of petals do not interact with the bow shock. It seems that a cowl design with a curved shape of the leading edge similar to the intersection line of the bow shock with the cowl is preferable.

The performance of the star-shaped inlet, shown in Figure 15, would be improved if a series of swept ramp injectors, which could add injectant inside the external part of the flow, were set along an intersection line of the bow shock with the cowling surface (dashed line in Figure 15). On one hand, they would speed up the mixing process and on the other hand, these ramp injectors could generate additional thrust. As a matter of fact, the front part of the cowling is usually inclined relative to the free flow (in Ref. [6] by ~24°) and the windward ramp injector surface is set at an angle where the effect of the telescope-shaped injector ([10]) is manifest. The schematic of one swept ramp injector as a trapezoid is displayed in Figure 15 by the dashed lines.

The new star-shaped inlet design differs essentially from the classical inlet scheme with conic forebody. As a matter of fact, the reflections from cowl and forebody occur in the flowfield of the internal inlet, where rarefaction waves, induced by the butt-ends of the "star" petals, can greatly reduce the oblique shock strength. As a result, the average Mach number in front of the normal shock will be insufficiently small for decelerated flow. On the other hand, the base pressure behind the petals is not low because of the fuel injected there. Therefore, counteraction of these two factors, possibly, eliminates the above-mentioned deficiency.

## V. CONCLUSIONS

Detailed analysis has shown that two proposed approaches: "SCRAMJET TELESCOPE INLET" and "SCRAMJET STAR-SHAPED INLET" have essential advantages with respect to the traditional designs. In particular, a star-shaped forebody at hypersonic speed has a lesser total drag compared with the equivalent cone. Also this design maintains fuel away from the boundary layer that contributes to prevention of early fuel combustion. These features plus the spatial configuration of the array injectors make the proposed design attractive as a potential for a scramjet inlet. Conduction of a numerical simulation, based on the NASA VULCAN code, is proposed in order to determine the optimal petal geometry, including its profile, number of petals and the dynamic pressure field in the wake of a star-shaped inlet. Numerical simulation of the flow past a star-shaped inlet with various numbers and types of injectors will also be conducted in order to select the optimum design in terms of uniform distribution of air-fuel mixture and minimum losses.

## VI. ACKNOWLEDGEMENTS

We would like to acknowledge the NASA Glenn and Langley Research Centers, especially Dr. Dennis M. Bushnell, Charles R. McClinton, and Carlos G. Rodriguez for interest and support to our research. This Research was partially conducted under the NASA grants: NAG-3-2422 and NCC-3-1037. We would like to thank Dr. Jay C. Hardin for his attention, interest in our research, review and useful suggestions.

## VII REFERENCES

1. Marble, F. E., Zukoski, E. E., et al., Shock Enhancement and Control of Hypersonic Mixing and Combustion, AIAA Paper 90-1981, July 1990 (see also AIAA Journal, v. 31, No 6, 1993).

2. Donohue, J. M., et al., Experimental and Numerical Study of Swept Ram Injector into a Supersonic Flowfield, AIAA Journal, v. 32, No 9, 1994.

3. Sislian, J. P., et al., Numerical Investigation of the Turbulent Mixing Performance of a Cantilevered Ramp Injector, AIAA Journal, v. 40, No 8, 2002.

4. Sislian, J. P., Parent, B., Impact of Axial Vortices on Mixing at a High Convective Mach Number, AIAA Journal, v. 41, No 7, 2003.

5. Tomioka, S., Jacobsen, L. S. and Schetz, J. A., Angled Injection Through Diamond-Shaped Orifices into Supersonic Stream, AIAA Paper 2001-1762.

6. Rodriguez, C. G., Computational Fluid Dynamics Analysis of the Central Institute of Aviation Motors/NASA Scramjet, J. of Propulsion and Power, v. 19, No. 4, July-August, 2003.

7. Seiner J.M., and Gilinsky, Nozzle Thrust Optimization while Reducing Jet Noise, 1995, 26th AIAA Fluid Dynamics Conference, June 19-22, 1995/San Diego, CA, 27p.

8. Seiner, J.M., and Gilinsky, M., Corrugated Nozzles for Acoustic and Thrust Benefits of Aircraft Engines, 1996, CEAS/AIAA Paper 96-1670, 2nd Joint CEAS/AIAA Aeroacoustics Conference, May 12-15, 1996/Penn.St. PA.

9. Seiner, J.M., Gilinsky, M., Undulated Nozzle for Enhanced Exit Area Mixing, US Patent #6,082,635, July 4, 2000.

10. Gilinsky, M., and Blankson, I.M., 2000, Internal Design Applications for Inlet and Nozzle Aeroperformance Improvement, AIAA Paper #00-3170, 36th AIAA/ASME/SAE/ASEE Joint Propulsion Conference, 17-19 June, 2000, Huntsville, Al.

11. Gilinsky, M., Blankson, I.M., Gromov V.G., and Sakharov V.I., Corrugated and composite nozzle-inlets for thrust and noise benefit. AIAA Paper N 2001-1893, Presented at the AIAA/NAL-NASDA-ISAS 10th International Space Planes and Hypersonic Systems

and Technology Conference, 24-27 April 2001, Kyoto, Japan.

12. Godunov, S.K. et al., 1976, Numerical Solution of Multidimensional Problems of Gas Dynamics, Moscow: Nauka, 1976, 400p.

13. Gromov, V.G., Sakharov, V.I., and Fateeva, E.I., 1999, Numerical Study of Hypersonic Viscous Chemically Reactive Gas Flow Past Blunt Bodies, Fluid Dynamics, v34, 1999, pp. 755-763.

14. Gaffney, R.L., Jr., White, J.A., Girimaji, S.S., and Drummond,J.P.,1992,Modeling Turbulence/ Chemistry Interactions Using Assumed PDF Methods, AIAA Paper #92-3638.

15. Gonor, A. L., The Spatial Shapes of Bodies of Minimum Drag at the High Supersonic Speeds, Report No. 5353. Publ.: Central Institute of Aviation Motors "CIAM", 1961, 72 p.

16. Gonor, A. L. and Chernyi, G. G., The Determination of Body Shapes of Minimum Drag Using Newton and Busemann Pressure Laws, Proc. of the Symposium on Extremal Problems in Aerodynamics, Boeing Scientific Research Laboratories, Seattle, Wash., 1962.

17. Gonor, A. L., On Three-Dimensional Bodies of Minimum Drag at Hypersonic Speed, J. of Applied Mathematics and Mechanics, v. 27, No. 1, Pergamon Press, 1963.

18. Gonor, A. L., Conical Bodies of Minimum Drag in Hypersonic Gas Flow, J. of Applied Mathematics and Mechanics, v. 28, No. 2, Pergamon Press, 1964.

19. Gonor, A. L., Determination of Shape of an Optimum Three-Dimensional Body with Allowance for Friction, Bulletin of Academy of Sciences, USSR, Mechanics, No. 4, 1965 (in Russian).

20. Miele, A. and Saaris G. R., On the Optimum Transversal Contour of a Body at Hypersonic Speed, Astronautica Acta, v. 9, No. 3, 1963.

21. Theory of Optimum Aerodynamic Shapes (Ed. A. Miele), An International Series of Monographs, v. 9, Academic Press, 1965.

22. Hayes, W. D. and Probstein, R. F., Hypersonic Flow Theory, Second Edition, An International Series of Monographs, v. 5, Academic Press, 1966.

23. Gonor, A. L., Shvets, A. I. and Kazakov, M. N., Total Drag of Star-Shaped Body at Hypersonic Speed, Fluid Dynamics Transactions, v. 4, pp. 225-229, Polish Academy of Sciences., Warsaw, 1969.

24. Gonor, A. L., Kazakov, M. N., and Shvets, A. I., Measurement of the Drag of a Star-Shaped Body in Supersonic Flow, Fluid Mechanics, v. 3, No. 1, Plenum Press, 1968.

25. Gonor, A. L., Kazakov, M. N., Shvets, A. I. and Shein, V. I., Aerodynamic Characteristics of Star-Shaped Bodies at Supersonic Velocities, Fluid Dynamics, v. 6, No. 1, Plenum Press, 1971.

26. Vedernikov, Yu. A., Gonor, A. L., Zubin, M. A. and Ostapenko, N. A., Aerodynamic Characteristics of Star-Shaped Bodies at Mach Numbers M = 3-5, Fluid Dynamics, v. 16, No. 4, pp. 559-563, Plenum Press, 1981.

27. Gonor, A. L., Zubin, M. A., Ostapenko, N. A., Chernyi, G. G. and Shvets, A. I., Aerodynamics of Star-Shaped Bodies at Supersonic Speeds, Proc. "Actual Problems of Mechanics", Publ.: Moscow University, 1984.

28. Zubin, M. A. and Ostapenko, N. A., Static Stability of Star-Shaped Conical Bodies in Supersonic Flow, Fluid Dynamics, v. 27, No. 6, Plenum Press, 1992.

29. Gonor, A. L., Shvets, A. I. and Kazakov, M. N., Some Results of the Supersonic Flow by V-shaped Wings, Fluid Dynamics Transactions, v. 5, Part II, pp. 97-106, Polish Academy of Sci., Warsaw, 1971.

30. Gonor, A. L. and Shvets, A. I., Flow Past V-Shaped Wings at Mach Number $M_{\infty}=4$, Fluid Dynamics, v. 2, No. 6, Plenum Press, 1967.